Experimental Demonstration of Ambiguous Staggered SAR with Waveform Alternation for Coastal Surveillance

Nertjana Ustalli, *Member, IEEE*, Maxwell Nogueira Peixoto, *Student Member, IEEE*, Thomas Kraus, Ulrich Steinbrecher, Gerhard Krieger, *Fellow*, *IEEE*, Michelangelo Villano, *Senior Member, IEEE*

***Abstract*—Maritime surveillance using synthetic aperture radar (SAR) calls for both wide swaths and high resolution. This enables monitoring of wide areas with high detection probabilities and low false alarm rates at short time intervals. Ambiguous SAR modes have proven effective for ship monitoring in remote offshore regions. They deliver high-resolution SAR images over wide swaths that can be effectively exploited for ship detection, even though they are corrupted by significant ambiguities of ships and sea clutter. Building upon the successful demonstration of the staggered ambiguous mode using TerraSAR-X, this paper presents the results of a further experimental acquisition, carried out near the Dutch coast, where an ultra-wide ground swath of 160 km is imaged at an azimuth resolution of 2.2 m by introducing in the staggered ambiguous mode alternation of up- and down-chirp waveforms. 79 small ships were detected in the data set, some of which even near the coast and despite the presence of first-order range ambiguities caused by land scatterers, as these ambiguities are very blurred and manifest as noise like disturbances. These results are of fundamental importance for incorporating the ambiguous modes into existing and future SAR systems as an efficient additional mode for ship monitoring, suitable for both open sea and coastal surveillance.**

***Index Terms*—Ambiguities, chirp, high-resolution wide-swath imaging, maritime monitoring, ship detection, synthetic aperture radar (SAR), staggered SAR, TerraSAR-X, waveforms.**

I. Introduction

Synthetic aperture radar (SAR) images have great potential for observing and monitoring the maritime environment, benefiting applications like maritime traffic control, pollution monitoring, fisheries, smuggling prevention, and defense purposes [1], [2], [3]. User requirements include persistence, high detection performance, and responsiveness. Mapping wider swaths improves the observation frequency, while higher resolution SAR images enhance the detection performance by providing more favorable statistics. On-board processing reduces the latency for improved responsiveness.

Manuscript received Month XX, 202X; revised Month XX, 202X; accepted Month XX, 202X. Date of publication Month XX, 202X; date of current version Month XX, 202X.

The authors are with the German Aerospace Center (DLR), Microwaves and Radar Institute Oberpfaffenhofen, 82234 Wessling, Germany (e-mail: nertjana.ustalli@dlr.de).

Color versions of one or more of the figures in this paper are available online at http://ieeexplore.ieee.org.
Digital Object Identifier XX.XXXX/TGRS.202X.XXXXXXX.

However, wide-swath coverage and high-resolution imaging pose contradicting requirements on the pulse repetition frequency (PRF). Controlling range ambiguities requires a pulse repetition interval (PRI) greater than the time needed to collect returns from the entire illuminated swath. A large PRI (low PRF) limits the unambiguous Doppler bandwidth and therefore the achievable azimuth resolution if azimuth ambiguities have to be controlled [4]. A wide swath can also be mapped with ScanSAR or Terrain Observation by Progressive Scans (TOPS), but the azimuth resolution is still impaired. Digital beamforming (DBF) and multiple aperture recording are promising techniques that overcome these limitations and achieve high-resolution wide-swath SAR imaging. However, they also involve higher system complexity and costs.

In [5], we have proposed two high-resolution wide-swath modes for ship monitoring that "tolerate" ambiguities and are suitable for offshore region surveillance: the low PRF mode, which tolerates azimuth ambiguities of the ships that might be recognized as artifacts, and the staggered (high PRF) ambiguous mode, which tolerates range ambiguities of the ships, as they are blurred and do not exceed the disturbance level. Both modes map wide swaths by using a wide elevation beam on both transmit and receive obtained through tapering [6]. In particular, the staggered ambiguous mode uses a sequence of distinct PRIs with a mean PRF greater than the Doppler bandwidth and has the advantage that range ambiguities of ships can be significantly blurred, thereby not exceeding the detection threshold, if proper PRI sequences are employed. A larger swath, but at a coarser azimuth resolution, can be imaged with a ScanSAR mode with six sub-swaths that tolerates azimuth ambiguities, as proposed by NovaSAR [7]. This, however, leads to the detection of only medium to large ships with a false alarm rate of 10^{-7}.

Already in [5], we showed that the ambiguous SAR modes enable the detection of small ships, i.e., of 21 m × 6 m size, by imaging a wide swath of up to 240 km with a probability of detection of at least 0.85, while also keeping the same false alarm rate as the aforementioned mode by NovaSAR, corresponding to one false alarm over a 1000 km^2 area. The ambiguous modes therefore achieve a swath similar to that of a ScanSAR mode and a resolution cell of 2 m^2, similar to that of a spotlight mode. For a ScanSAR mode that images the same swath (100 km ground swath as in TerraSAR-X) with a coarser resolution of 5 m × 18.5 m (ground range × azimuth) as in

TerraSAR-X, which corresponds to a resolution cell area of 92.5 m², the probability of detection, assuming the same ship size (the ship is expected to occupy one or at most two resolution cells in this case) and false alarm rate as in the ambiguous modes would be less than 0.3 [5].

Ref. [8] reports on an experimental TerraSAR-X acquisition in staggered ambiguous mode imaging a ground swath of 110 km in open sea (about 27 km far from the coast) with 2.2 m azimuth resolution performed over the North Sea. Data have been processed and the detection results have been successfully validated using automatic identification system data. The impact of the TerraSAR-X technical limitations on the selection of non-optimal system parameters for ship detection application, such as the PRI sequence, pulse length, and the chirp bandwidth has been thoroughly discussed in [8]. The use of a non-optimal PRI sequence has resulted in range ambiguities from ships still being above the detection threshold and their specific signature due to the PRI variation has still allowed for discrimination between the ships and their ambiguities.

Building upon the findings presented in [8], this work reports the results of a further experimental TerraSAR-X acquisition conducted in the North Sea and including part of the Dutch coast. The acquisition features the staggered ambiguous mode jointly with alternating up- and down-chirps. This will enable additional smearing of the first (and all odd) range ambiguities associated with large ships and land scatterers and therefore ship monitoring in coastal areas. Furthermore, there will be fewer false alarms resulting from the first-order range ambiguities of large ships, particularly in scenarios where selecting an optimal PRI sequence is not feasible, as observed in the TerraSAR-X experiment discussed in [8]. Please note that the low PRF mode in [5] cannot be exploited for coastal monitoring.

This letter provides an overview of the proposed mode, explains how the TerraSAR-X experiment was conducted, describes the associated data processing, and examines the detection of ships near the coast in this complex scenario. This analysis considers the challenges posed by range ambiguities originating from land scatterers.

II. Staggered Ambiguous Mode with Alternating Up- and Down-Chirps

The staggered ambiguous mode of [5] and the staggered SAR system employing DBF of [9] exhibit notable differences, which are discussed in [8]. In the staggered ambiguous mode with alternating up- and down-chirps, a wide elevation transmit beam illuminates a wide swath and the radar echoes are collected with the same wide beam used in transmit.

The upper part of Fig. 1 depicts the transmission and reception of radar echoes for the simplified case of a sequence of $M = 5$ PRIs with a linear decreasing trend. The transmitted pulses, separated by varying PRIs, and consisting of alternated up- and down-chirps, are displayed on a time axis in the upper part of the upper panel. Each transmitted pulse is represented by a different color with the circled number indicating the pulse index; the up-chirp and down-chirp pulses are denoted with the symbols U and D, respectively. Immediately below, the received echoes corresponding to the first two transmitted pulses are shown on the same time axis. The radar echoes from the sea clutter are displayed with the same colors as the corresponding transmitted pulses. The radar echo return from a ship at a slant range R_0 (for simplicity, we assume the ship is not moving) overlaps to the echo return from the sea clutter and it is marked in red, with the upper circled number followed by the symbol U or D indicating the corresponding transmitted pulse. It is important to note that while we receive the desired radar echo of the ship at slant range R_0 from pulse number 0, marked in red, we will also receive an ambiguous return from pulse number 1, shown in white with upper circled number 1 and symbol D. This happens because the receive echo window is typically much shorter than the duration of the radar echo from the illuminated swath. This is also true for the sea clutter returns, which will overlap.

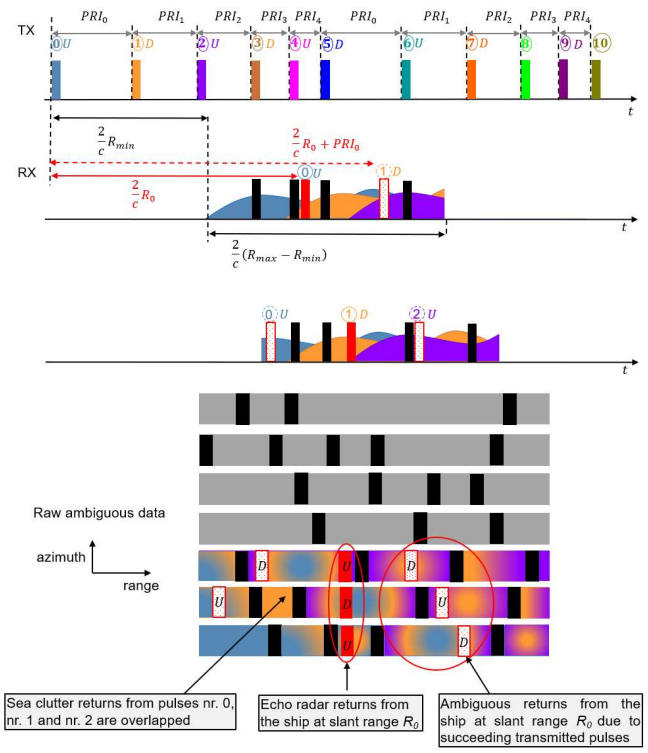

Fig. 1 Top: Transmitted pulses and corresponding received echoes. Bottom: Raw data obtained by rearranging side by side the received echoes.

The received echoes are then rearranged, i.e., shifted at the same reception time as shown in the bottom panel of Fig. 1. As a result, the received radar echoes from the ship are at the same slant range R_0 for all range lines, while its ambiguous returns are located at different ranges for different range lines, as the time difference between the transmit pulses continuously varies.

Please note that this also applies to the sea clutter returns, which consist of the sum of the non-ambiguous sea clutter component and the range-ambiguous sea clutter components from different pulses, as their duration in the received radar echo is longer than the PRIs. Following the range compression of the rearranged data, achieved by alternating up and down chirps in Fig. 1, the ship at the slant range R_0 will be focused in range. In contrast, its first order range ambiguity (along with

all the odd order range ambiguities) will be blurred in range during the range compression operation. The blurring effect occurs because of the mismatch between the ambiguous returns, alternating between down- and up-chirps, and the reference signal, alternating between up- and down-chirps in the example shown in Fig. 1. The blurring or smearing factor of the odd ambiguities in range is proportional to the compression ratio of the transmitted chirp [10]. Furthermore, after azimuth compression, the ambiguous energy of both even and odd order range ambiguities, due to PRI variation, is incoherently integrated and will spread almost uniformly across the whole Doppler spectrum [10]. The same applies to sea clutter echoes or land scatterers. This results in an increase in the disturbance level in the region affected by the ambiguities, which must be considered when selecting the threshold to detect the ships.

Due to the radar's inability to receive while transmitting, some "blind areas" will be present on the received data, which are marked in black in the upper and bottom panel of Fig. 1. As the PRI is continuously varied, the locations of the blind areas will be different for each range line, as they are related to the time distances between the transmitted pulses.

III. TerraSAR-X Experiment

TerraSAR-X is a conventional phased-array SAR that can be operated with continuously varying PRI, because it has 512 different PRIs and can be commanded to transmit pulses based on a sequence of M distinct PRIs that then repeats periodically, as demonstrated in [9].

An area in the North Sea along the Dutch coast was selected as test site for the demonstration. The chosen elevation beam allows imaging a 160-km ground swath with minimum and maximum look angles of 53.08° and 57.29°, respectively. The 160-km ground swath is not defined by the 3-dB antenna beamwidth, but extends beyond it, as TerraSAR-X still provides adequate noise equivalent sigma zero for this specific mode, ensuring a sufficient signal-to-noise ratio for effective ship detection across the wide swath. Fig. 2 shows the test site, with the red rectangle representing the 66-km ground swath defined by the 3-dB antenna beamwidth. The green rectangle outlines the 160 km ground swath area of the acquired SAR image, which includes a portion of the Dutch coast.

Once the beam has been selected, other system parameters such as the PRI sequence, the pulse length τ, and the chirp bandwidth B_r, have to be chosen to ensure the best ship detection performance while respecting the TerraSAR-X technological constraints. The three main constraints of TerraSAR-X include the maximum echo window length, the maximum allowed duty cycle, and the limited number of selectable PRIs. For a pulse length of 45 μs and a chirp bandwidth of 100 MHz, it is possible to design a sequence of M = 43 PRIs that satisfies all the constraints, as for the experiment in [8], with a mean PRF of the sequence of 3525 Hz greater than the 3 dB Doppler bandwidth (2807 Hz) and mean duty cycle of 16.1%. A ground range resolution of 1.75 m at near range and an azimuth resolution of 2.2 m are achieved, if no weighting windows are applied within the processing. The expected impulse responses of the first-order range ambiguity for the two cases (same waveform and waveform alternation) and the aforementioned parameters show a difference in the intensity of the maximum pixel of about 13 dB.

The TerraSAR-X experimental acquisition in staggered ambiguous mode with additional up- and down-chirp alternation has been carried out on July 31, 2023 over the North Sea. The sequence of 43 PRIs is repeated 2800 times. The echoes, received by the radar between consecutive transmitted pulses, have different duration, as different PRIs are employed. Unlike in a SAR with constant PRI, the first samples of the received echoes correspond in a staggered SAR system to different slant ranges. Those echoes have therefore to be rearranged in a two-dimensional matrix with coordinates slant range and azimuth. This rearrangement associates each sample of radar echo with its corresponding range.

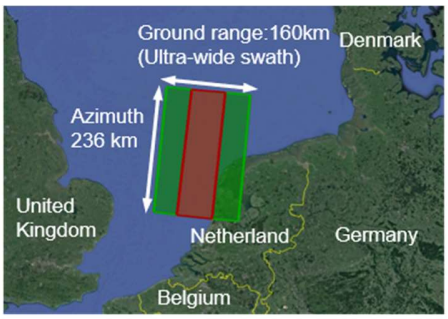

Fig. 2 North Sea test site selected for the experimental acquisition. The green rectangle delimits the 160-km ground swath area of the acquired SAR image, while the red rectangle delimits the area within the 66-km ground swath from the 3-dB antenna beamwidth.

Please note that each received echo contains not only the desired return, but also the returns of preceding and succeeding pulses as they arrive back at the radar at the same time. After rearrangement, range compression is performed using alternating up- and down-chirps. Subsequently, the data are resampled on a uniform grid, following the procedures outlined in [13]. It is important to note that in this acquisition, due to the alternation of up- and down-chirps on transmit, azimuth resampling on a uniform grid cannot be performed on the rearranged raw data, but only after range compression, unlike in staggered SAR systems transmitting always the same waveforms [13]. Range cell migration correction and azimuth compression are then performed.

The detection of ships includes two main stages. In the first stage, the overall image intensity is compared to an adaptive threshold that depends on the variable background level, i.e., it is about 10 dB higher than the average intensity evaluated over a window extending over twice the pulse width in range and over the synthetic aperture in azimuth. In particular, absolute thresholds ranging from 3.8 dB to 11 dB (on the radiometrically-calibrated image) have been used in this specific acquisition to guarantee approximately constant false alarm rate for a given ship size. The detection probability will be therefore variable across the scene. Pixels surpassing the threshold are identified as potentially belonging to a ship. In the second stage, the Density-Based Spatial Clustering of Applications with Noise (DBSCAN) algorithm of [14] is employed to cluster pixels exceeding the threshold and belonging to the same ship, as also done in [8].

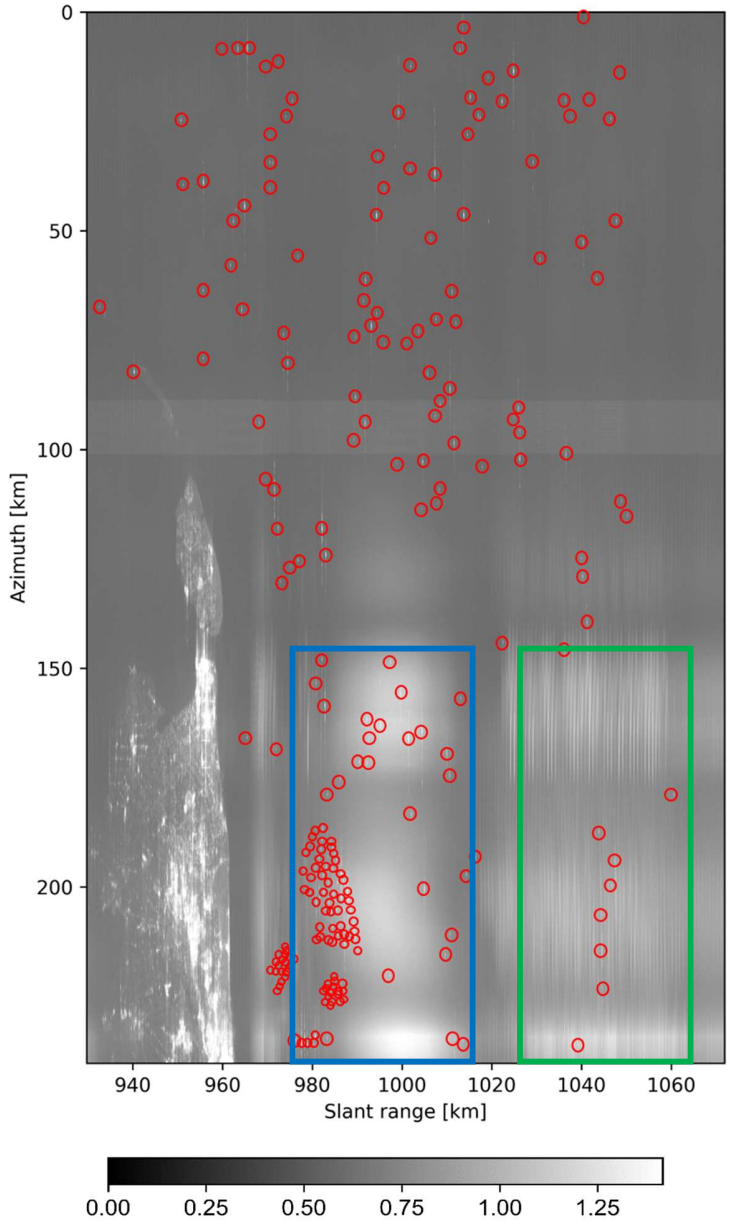

Fig 3 Intensity of the focused image acquired by TerraSAR-X in staggered ambiguous mode with alternating up- and down-chirps over the full scene with superimposed red circles indicating the detected ships. The blue rectangle and the green rectangle highlight the first-order and the second-order range ambiguities from the coast.

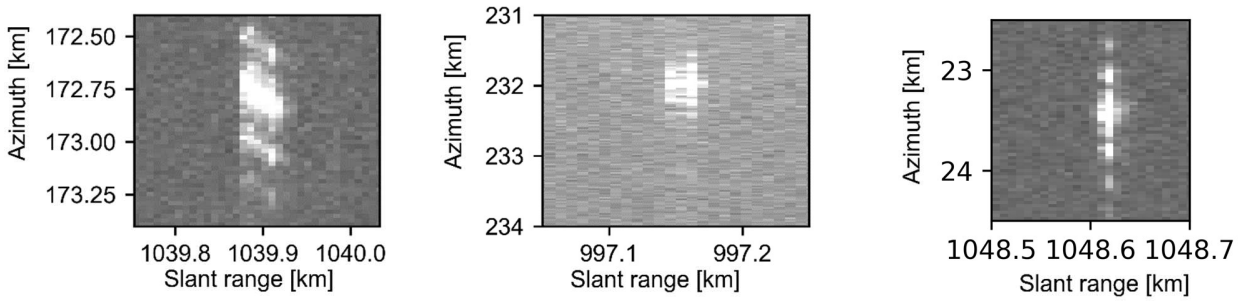

Fig 4 Zoom around medium and small ships within the scene (a) zoom around a medium ship at far range, (b) zoom around a small ship overlapped to the first-order range ambiguity of land scatterers and (c) zoom around a small ship at far range. The same color scale as in Fig. 3 is used.

IV. Results

Fig. 3 shows the intensity of the focused data for the entire scene, covering an area of about 37 760 km^2, where the strong returns from ships along with the coastline and the first- and second-order range ambiguities from the coast are visible. We show with a red circle the centroid of each detected ship. The blue and green rectangles highlight the areas affected by first- and second-order range ambiguities of land scatterers, respectively. A total of 275 ships have been detected in the full scene, namely 79 small ships (ship length $\leq$ 25 m), 109 medium ships (25 m < ship length $\leq$ 150 m), and 87 large ships (ship length > 150 m). Fig. 4 provides a closer look of three medium and small ships within the scene that exceed the detection threshold. Fig. 4 (b) shows a small ship overlapped to the first order range ambiguities from the land scatterers inside the blue rectangle shown in Fig. 3. The impulse response has some higher sidelobes due to the variable PRI and missing samples in azimuth, but this does not prevent or significantly degrade the detection of ships. The sidelobes in azimuth could have been avoided using a much larger mean PRF (not implementable by the TerraSAR-X system as discussed in detail in [9]), but this would have also resulted in a much higher ambiguous clutter level.

V. Conclusions and Outlook

An experimental TerraSAR-X acquisition in staggered ambiguous mode with alternating up- and down-chirps imaging a ground swath of 160 km with 2.2 m azimuth resolution has been performed. It is shown that the proposed mode is effective for both open sea and coastal surveillance. The proposed mode could be part of an observation strategy, where an ultrawide swath is observed using the ambiguous mode, and the acquired data (and the location of the detected ships) trigger a second acquisition, e.g., in spotlight mode as hinted in [17].

In this experiment, the up- and down-chirp alternation led to full blurring of the first-order range ambiguity, whereas the second-order was not totally blurred. Utilizing OFDM waveforms, as e.g. in [15], can blur all desired orders of range ambiguities. This is particularly desired, when as in this experiment an optimal PRI sequence cannot be employed.

Another interesting option is refocusing the range ambiguities of large ships (using the proper waveforms and PRI sequence in the matched filtering) and removing them following an approach similar to the one proposed in [16]. Furthermore, employing advanced detection techniques exploiting machine learning approaches could automate the rejection of artifact-induced false alarms. This could be matter of future investigations.

Finally, the introduction of waveform alternation, due to the consequent range ambiguity blurring, facilitates the adoption of ambiguous staggered SAR data to land-based applications, such as deformation monitoring using permanent scatterers interferometry.

References

[1] J. Krecke, M. Villano, N. Ustalli, A. C. M. Austin, J. E. Cater, and G. Krieger, “Detecting ships in the New Zealand exclusive economic zone: Requirements for a dedicated smallsat SAR mission,” IEEE J. Sel. Topics Appl. Earth Observ. Remote Sens., vol. 14, pp. 3162–3169, 2021.

[2] M. Migliaccio, F. Nunziata, A. Montuori and R. L. Paes, "Single-Look Complex COSMOSkyMed SAR Data to Observe Metallic Targets at Sea," in IEEE Journal of Selected Topics in Applied Earth Observations and Remote Sensing, vol. 5, no. 3, pp. 893-901, June 2012,

[3] S. Brusch, S. Lehner, T. Fritz, M. Soccorsi, A. Soloviev and B. van Schie, "Ship Surveillance with TerraSAR-X," in IEEE Transactions on Geoscience and Remote Sensing, vol. 49, no. 3, pp. 1092-1103, March 2011.

[4] C. Curlander and R. N. McDonough, Synthetic Aperture Radar Systems and Signal Processing (Wiley Series in Remote Sensing), Boulder, Colorado: Pocket Ventures LLC, 1991.

[5] N. Ustalli, M. Villano, “High-Resolution Wide-Swath Ambiguous Synthetic Aperture Radar Modes for Ship Monitoring,” Remote Sensing, vol. 14, no. 13, p. 3102, Jun. 2022.

[6] M. Villano, G. Krieger, and A. Moreira, “Advanced spaceborne SAR systems with planar antenna,” 2017 IEEE Radar Conference (RadarConf), Seattle, WA, USA, 2017, pp. 0152-0156.

[7] M. Cohen, A. Larkins, P. L. Semedo and G. Burbidge, “NovaSAR-S low cost spaceborne SAR pay-load design, development and deployment of a new benchmark in spaceborne radar,” 2017 IEEE Radar Conference (RadarConf), Seattle, WA, USA, 2017, pp. 0903-0907.

[8] N. Ustalli, M. N. Peixoto, T. Kraus, U. Steinbrecher, G. Krieger, and M. Villano, “Experimental Demonstration of Staggered Ambiguous SAR Mode for Ship Monitoring with TerraSAR-X,” IEEE Transactions on Geoscience and Remote Sensing, vol. 61, pp. 1-16, 2023.

[9] M. Villano, G. Krieger, M. Jäger, and A. Moreira, “Staggered SAR: Performance Analysis and Experiments with Real Data,” IEEE Transactions on Geoscience and Remote Sensing, vol. 55, no. 11, pp. 6617-6638, Nov. 2017.

[10] N. Ustalli and M. Villano, “Impact of Ambiguity Statistics on Information Retrieval for Conventional and Novel SAR Modes,” 2020 IEEE Radar Conference (RadarConf20), Florence, Italy, 2020, pp. 1-6.

[11] M. Villano and M. N. Peixoto, “Characterization of nadir echoes in multiple-elevation-beam SAR with constant and variable pulse repetition interval,” IEEE Trans. Geosci. Remote Sens., vol. 60, 2022.

[12] N. Ustalli, G. Krieger, and M. Villano, “A low-power, ambiguous synthetic aperture radar concept for continuous ship monitoring,” IEEE J. Sel. Topics Appl. Earth Observ. Remote Sens., vol. 15, pp. 1244–1255, 2022.

[13] M. Villano, G. Krieger, and A. Moreira, “A Novel Processing Strategy for Staggered SAR,” IEEE Geoscience and Remote Sensing Letters, vol. 11, no. 11, pp. 1891-1895, Nov. 2014.

[14] M. Ester, H. -P. Kriegel, J. Sander, and X. Xu, “A density-based algorithm for discovering clusters in large spatial databases with noise”, in: E. Simoudis, J. Han, U.M. Fayyad (Eds.), Proceedings of the Second International Conference on Knowledge Discovery and Data Mining, Port Land, OR, AAAI, Menlo Park, CA, 1996, pp. 226–231.

[15] W.-Q. Wang, “Mitigating Range Ambiguities in High-PRF SAR With OFDM Waveform Diversity,” in IEEE Geoscience and Remote Sensing Letters, vol. 10, no. 1, pp. 101-105, Jan. 2013.

[16] M. Villano, G. Krieger and A. Moreira, “Waveform-Encoded SAR: A Novel Concept for Nadir Echo and Range Ambiguity Suppression,” EUSAR 2018; 12th European Conference on Synthetic Aperture Radar, Aachen, Germany, 2018, pp. 1-6.

[17] G. Krieger, N. Gebert and A. Moreira, "Multidimensional Waveform Encoding: A New Digital Beamforming Technique for Synthetic Aperture Radar Remote Sensing," in IEEE Transactions on Geoscience and Remote Sensing, vol. 46, no. 1, pp. 31-46, Jan. 2008.